

Scattering of universal fermionic clusters in the resonating group method

Pascal Naidon¹, Shimpei Endo², and Antonio M. García-García³

¹*RIKEN Nishina Centre, RIKEN, Wako, 351-0198 Japan*

²*Laboratoire Kastler-Brossel, École Normale Supérieure, 24 rue Lhomond, 75231 Paris, France and*

³*University of Cambridge, Cavendish Laboratory,
JJ Thomson Avenue, Cambridge, CB3 0HE, UK*

(Dated: September 25, 2021)

Mixtures of polarised fermions of two different masses can form weakly-bound clusters, such as dimers and trimers, that are universally described by the scattering length between the heavy and light fermions. We use the resonating group method to investigate the low-energy scattering processes involving dimers or trimers. The method reproduces approximately the known particle-dimer and dimer-dimer scattering lengths. We use it to estimate the trimer-trimer scattering length, which is presently unknown, and find it to be positive.

I. INTRODUCTION

In the last decade, the use of controlled Feshbach resonances in ultra-cold atom experiments have enabled the study of low-energy quantum systems of particles interacting with large scattering lengths. Close to a Feshbach resonance, the interparticle scattering length is much larger than the range of interparticle forces. As a result, the low-energy properties of these systems are universal, in the sense that they depend only upon a few parameters, such as the scattering length [1], and the three-body parameter [2, 3] in systems exhibiting the Efimov effect [4–6]. Moreover, close to Feshbach resonances, atoms can be associated into clusters of universal character: diatomic molecules called Feshbach molecules that are a realisation of universal dimers [7–14], triatomic molecules that are a realisation of Efimov states [15–17]. Theory predicts the existence of a variety of other universal clusters of larger number of particles [18–20] that are expected to be observed experimentally in the future [21].

The few-body properties, in particular the scattering properties of clusters, can play a crucial role in the identification and stability of the many-body ground states of these systems. For instance, the stability of a gas of universal dimers made of fermions was observed [8, 10–14] and explained theoretically [22, 23] by exact four-body calculations for two scattering dimers.

Although it is sometimes feasible to calculate exactly the wave function of an N -body cluster [4, 24], the exact computation of the scattering properties of two clusters is generally out of reach for $N \geq 3$. In the context of nuclear and sub-nuclear physics, a broad array of approximation schemes have been successfully developed to address similar problems. One of the leading techniques is the so-called Resonating Group Method (RGM), introduced by Wheeler [25], to study light nuclei, such as ^{16}O and ^8Be , modelled as clusters of α particles. Since then, it has been employed in a variety problems including the scattering of light nuclei, the stability of light nuclei to external nucleon scattering and nuclear particles [26, 27]. More recently, it has been used [28–30] to study low-energy scattering, and bound states, of baryon-baryon and

other multi-quark cluster configurations.

In the single-channel approximation, the RGM constructs the low-energy scattering wave function of two or more scattering clusters from the wave functions of the individual clusters, while preserving the full antisymmetrization of wave functions. This gives an effective potential between the clusters that can be used to treat scattering as well as bound states. It is especially accurate in situations in which single clusters are not strongly altered by the scattering process. Here, we propose to apply this method to the low-energy scattering of universal fermionic clusters that are relevant to ultra-cold atoms close to Feshbach resonances.

The paper is organised as follows. In section II, we review the essence of the RGM. In section III, we apply it to universal clusters whose scattering properties are known. In section IV, we apply the RGM to the yet unknown scattering of universal trimers.

II. THE RESONATING GROUP METHOD

A. General formalism

Let us consider the scattering between a cluster A of n particles and a cluster B of $N - n$ particles. It is assumed that the wave functions $\phi_A(1, 2, \dots, n)$ and $\phi_B(n + 1, n + 2, \dots, N)$ of these clusters are known. In the single-channel RGM, the N -body wavefunction Ψ describing the scattering process is constructed as the antisymmetrised product of the cluster wave functions and a wave function $\psi(\mathbf{R})$ for the relative motion between the two clusters:

$$\Psi = \mathcal{S} [\phi_A(1, 2, \dots, n) \phi_B(n + 1, n + 2, \dots, N) \psi(\mathbf{R})]. \quad (1)$$

Here, \mathcal{S} denotes the symmetrisation (or antisymmetrisation) operator that symmetrises (or antisymmetrises) the wave function under the exchange of identical particles. Symmetrisation is performed for bosonic particles, whereas antisymmetrisation is performed for fermionic particles. The vector \mathbf{R} describes the relative position between the centres of mass of the two clusters. The idea behind this approximation is that the structure of the two clusters is not much altered during the collision, and the two clusters mix

only through the exchange of identical particles.

The purpose of the RGM is to determine the wave function $\psi(\mathbf{R})$ for the relative motion of the clusters. This is done by applying the variation principle to the average quantity,

$$\langle \Psi | H - \mathcal{E} | \Psi \rangle, \quad (2)$$

where H is the total hamiltonian and \mathcal{E} is the total energy of the system. Requiring ψ to extremise the above quantity implies that for an infinitesimal variation $\delta\psi$ around ψ we have

$$\langle \mathcal{S}[\phi_A \phi_B \delta\psi] | H - \mathcal{E} | \mathcal{S}[\phi_A \phi_B \psi] \rangle + \text{c.c.} = 0.$$

The variations $\delta\psi$ and its complex conjugate $\delta\psi^*$ can be formally taken as independent variations, resulting in the following Euler-Lagrange equation of motion,

$$\langle \mathcal{S}[\phi_A \phi_B] | H - \mathcal{E} | \mathcal{S}[\phi_A \phi_B \psi] \rangle = 0, \quad (3)$$

which can be simplified as

$$\langle \phi_A \phi_B | H - \mathcal{E} | \mathcal{S}[\phi_A \phi_B \psi] \rangle = 0. \quad (4)$$

since the total hamiltonian H is invariant under the exchange of identical particles.

The hamiltonian H consists of kinetic operators t_i for each particle and pairwise interaction terms V_{ij} for each pair of particles,

$$H = \sum_{i=1}^N t_i + \sum_{i<j}^N V_{ij} - t_c. \quad (5)$$

We have subtracted the kinetic operator t_c for the centre of mass, since it can be eliminated from the problem. The hamiltonian can be rewritten as

$$H = H_A + H_B + T_{\mathbf{R}} + V_{AB}, \quad (6)$$

where H_A and H_B denote the internal hamiltonian of each cluster A and B, $T_{\mathbf{R}}$ denotes the kinetic operator for the relative motion of the two clusters, and V_{AB} is the sum of interactions between the two clusters. The wave functions ϕ_A and ϕ_B are eigenstates of H_A and H_B with eigenvalues E_A and E_B , i.e.

$$H_A \phi_A = E_A \phi_A \quad \text{and} \quad H_B \phi_B = E_B \phi_B. \quad (7)$$

There are two ways this can be used to simplify the equation of motion Eq. (4). Either one applies the hamiltonian to the wave functions ϕ_A and ϕ_B on the right-hand side, or to the wave functions ϕ_A and ϕ_B on the left-hand side. We refer to these two equivalent procedures as the RGM1 and RGM2. Although they result in formally different equations, their solutions are the same.

In the RGM1, one writes

$$\langle \phi_A \phi_B | \mathcal{S}[(H - \mathcal{E})\phi_A \phi_B \psi] \rangle = 0 \quad (8)$$

and using Eqs. (6) and (7)

$$\langle \phi_A \phi_B | \mathcal{S}[(T_{\mathbf{R}} + V_{AB} - E)\phi_A \phi_B \psi] \rangle = 0, \quad (9)$$

where $E = \mathcal{E} - E_A - E_B$ is the scattering energy between the two clusters. The symmetrisation operator \mathcal{S} can be written as $\mathcal{S} = \hat{1} + \mathcal{S}'$, i.e. the action of \mathcal{S} gives one term leaving the wave function unchanged, and other terms where particles are exchanged. Thus, Eq. (9) can be written as

$$\boxed{(1 - K) \cdot (T_{\mathbf{R}} - E)\psi + V_D \psi + V_{EX1} \cdot \psi = 0} \quad (10)$$

where we have introduced a local potential V_D called the direct potential,

$$V_D(\mathbf{R}) = \langle \phi_A \phi_B | V_{AB} | \phi_A \phi_B \rangle, \quad (11)$$

a non-local potential V_{EX1} called the exchange potential,

$$\begin{aligned} V_{EX1} \cdot \psi &= \int d^3 \mathbf{R}' V_{EX1}(\mathbf{R}, \mathbf{R}') \psi(\mathbf{R}') \\ &= \langle \phi_A \phi_B | \mathcal{S}'[V_{AB} \phi_A \phi_B \psi] \rangle, \end{aligned} \quad (12)$$

and a non-local operator K called the exchange kernel,

$$\begin{aligned} K \cdot \psi &= \int d^3 \vec{R}' K(\mathbf{R}, \mathbf{R}') \psi(\mathbf{R}') \\ &= -\langle \phi_A \phi_B | \mathcal{S}'[\phi_A \phi_B \psi] \rangle. \end{aligned} \quad (13)$$

In the RGM2, one applies the hamiltonian Eq. (6) to the wave functions $\phi_A \phi_B$ on the left-hand side of Eq. (4), using Eq. (7). This gives

$$\langle \phi_A \phi_B | (T_{\mathbf{R}} + V_{AB} - E) \mathcal{S}[\phi_A \phi_B \psi] \rangle = 0, \quad (14)$$

which can be written as

$$\boxed{(T_{\mathbf{R}} - E)(1 - K) \cdot \psi + V_D \psi + V_{EX2} \cdot \psi = 0} \quad (15)$$

where the exchange potential V_{EX2} is defined by

$$\begin{aligned} V_{EX2} \cdot \psi &= \int d^3 \vec{R}' V_{EX2}(\vec{R}, \vec{R}') \psi(\vec{R}') \\ &= \langle \phi_A \phi_B | V_{AB} \mathcal{S}'[\phi_A \phi_B \psi] \rangle. \end{aligned} \quad (16)$$

Hence, the RGM consists in calculating the potentials V_D , V_{EX} and kernel K , and solving the equation for the relative motion between the two clusters, either Eq. (10) or (15). This is of course a great simplification over solving the full N -body equation. Nonetheless, the determination of V_D , V_{EX} and K involve $3(n-1) + 3(N-n-1) = 3(N-2)$ -dimensional integrals whose computation may be costly for large N .

B. RGM with contact interactions

In the following, we apply the RGM to the scattering of universal clusters. Their universal character is described by the zero-range theory, which corresponds to the limit of the range of interaction being much smaller than the s -wave scattering length a . In this

limit, the interaction potential V_{ij} between two particles appearing in Eq. (5) and included in the term V_{AB} in Eq. (6) can be approximated by a contact potential,

$$V_{ij}(\mathbf{r}) = g\delta^3(\mathbf{r})\frac{\partial}{\partial r}r. \quad (17)$$

with the coupling constant

$$g = \frac{4\pi\hbar^2 a}{2\mu}. \quad (18)$$

Here, μ is the reduced mass of the two interacting particles, and $\partial/\partial r r$ is an operator regularising the $1/r$ divergence of the wave function when particles come into contact ($r = 0$). This potential binds two particles only for $a > 0$, and we restrict our consideration to this case throughout this paper.

The presence of the three-dimensional Dirac delta function in the potential Eq. (17) reduces by three the dimensionality of the integrals. The dimensionality of the integrals Eqs. (11), (12), and (16), for V_D , V_{EX1} and V_{EX2} , is thus reduced to $3(N - 3)$.

C. Partial-wave expansion

To proceed further, one can perform a partial-wave expansion in spherical harmonics $Y_{\ell m}$ in the RGM1 and RGM2 equations. The relative wave function is expanded as

$$\psi(\mathbf{R}) = \sum_{\ell m} \frac{1}{R} \psi_{\ell m}(R) Y_{\ell m}(\hat{R}), \quad (19)$$

where \hat{R} denotes the orientation of \mathbf{R} . Then, the RGM1 equation, Eq. (10), becomes the following set of coupled equations:

$$\begin{aligned} (T_R^\ell - E) \psi_{\ell m}(R) + \sum_{\ell' m'} V_D^{\ell m, \ell' m'}(R) \psi_{\ell' m'}(R) & \quad (20) \\ - \sum_{\ell' m'} \int_0^\infty dR' K^{\ell m, \ell' m'}(R, R') (T_{R'}^{\ell'} - E) \psi_{\ell' m'}(R') \\ + \sum_{\ell' m'} \int_0^\infty dR' V_{EX1}^{\ell m, \ell' m'}(R, R') \psi_{\ell' m'}(R') & = 0 \end{aligned}$$

and the RGM2 equation, Eq. (15), becomes the set of coupled equations

$$\begin{aligned} (T_R^\ell - E) \psi_{\ell m}(R) + \sum_{\ell' m'} V_D^{\ell m, \ell' m'}(R) \psi_{\ell' m'}(R) & \quad (21) \\ - \sum_{\ell' m'} \int_0^\infty dR' (T_{R'}^\ell - E) K^{\ell m, \ell' m'}(R, R') \psi_{\ell' m'}(R') \\ + \sum_{\ell' m'} \int_0^\infty dR' V_{EX2}^{\ell m, \ell' m'}(R, R') \psi_{\ell' m'}(R') & = 0 \end{aligned}$$

with the kinetic energy operator

$$T_R^\ell = \frac{\hbar^2}{2\mu_N} \left(-\frac{d^2}{dR^2} + \frac{\ell(\ell+1)}{R^2} \right), \quad (22)$$

where μ_N is the reduced mass of the two clusters, and

$$V_D^{\ell m, \ell' m'}(R) = \int d^2 \hat{R} Y_{\ell m}^*(\hat{R}) V_D(\mathbf{R}) Y_{\ell' m'}(\hat{R}), \quad (23)$$

$$\begin{aligned} K^{\ell m, \ell' m'}(R, R') & = RR' \int d^2 \hat{R} d^2 \hat{R}' \\ & Y_{\ell m}^*(\hat{R}) K(\mathbf{R}, \mathbf{R}') Y_{\ell' m'}(\hat{R}'), \end{aligned} \quad (24)$$

$$\begin{aligned} V_{EX}^{\ell m, \ell' m'}(R, R') & = RR' \int d^2 \hat{R} d^2 \hat{R}' \\ & Y_{\ell m}^*(\hat{R}) V_{EX}(\mathbf{R}, \mathbf{R}') Y_{\ell' m'}(\hat{R}'). \end{aligned} \quad (25)$$

The dimensionality of integration in Eqs. (23), (24) and (25) is, respectively, $3(N - 2) - 1$, $3(N - 2) + 1$, and $3(N - 2) - 2$.

D. Local approximation

It turns out, as we shall see in the cases treated below, that the contribution from the non-local kernel K is often small and may be neglected. Moreover, in some cases, the exchange potentials $V_{EX1}^{\ell m, \ell' m'}$ and $V_{EX2}^{\ell m, \ell' m'}$ are nearly local and may be approximated by the local potentials

$$V_{EX \text{ local}}^{\ell m, \ell' m'}(R) = \int_0^\infty dR' V_{EX}^{\ell m, \ell' m'}(R, R'). \quad (26)$$

Neglecting K and using the local form Eq. (26) of the exchange potentials constitute the local RGM approximation. In this approximation, RGM1 and RGM2 equations have the form of conventional Schrödinger equations:

$$\boxed{(T_R^\ell - E) \psi_{\ell m}(R) + \sum_{\ell' m'} V_1^{\ell m, \ell' m'}(R) \psi_{\ell' m'}(R) = 0} \quad (27)$$

$$\boxed{(T_R^\ell - E) \psi_{\ell m}(R) + \sum_{\ell' m'} V_2^{\ell m, \ell' m'}(R) \psi_{\ell' m'}(R) = 0} \quad (28)$$

where $V_1^{\ell m, \ell' m'} = V_D^{\ell m, \ell' m'} + V_{EX1 \text{ local}}^{\ell m, \ell' m'}$, and $V_2^{\ell m, \ell' m'} = V_D^{\ell m, \ell' m'} + V_{EX2 \text{ local}}^{\ell m, \ell' m'}$.

Unlike the RGM1 and RGM2 equations, Eqs. (20) and (21), the local RGM1 and RGM2 equations, Eq. (27) and (28), are not equivalent. Nevertheless, they often yield similar results as we shall see in the following sections.

E. Scattering length and scattering volume

After solving the RGM equations in partial waves, Eq. (20) or (21), or their local-potential approximation, Eq. (27) or (28), one obtains the partial-wave components $\psi_{\ell m}(R)$ of the relative wave function ψ .

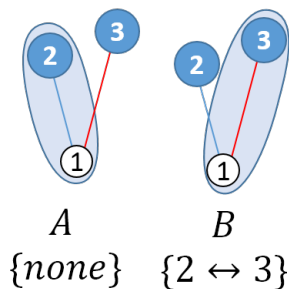


Figure 1: Schematic representation of the two permutations of identical fermions between a dimer and a fermion.

For zero scattering energy ($E = 0$), one can extract the partial-wave scattering lengths from these components.

From the s -wave component $\psi_{00}(R) \propto R + O(1)$ for $R \rightarrow \infty$, one obtains the s -wave scattering length,

$$a = \lim_{R \rightarrow \infty} R - \frac{\psi_{00}(R)}{\psi'_{00}(R)}, \quad (29)$$

and from the p -wave component $\psi_{1m}(R) \propto R^2 + O(1/R)$, one obtains the p -wave scattering volume,

$$v = \lim_{R \rightarrow \infty} \frac{R^3}{3} \frac{R\psi'_{1m}(R) - 2\psi_{1m}(R)}{R\psi'_{1m}(R) + \psi_{1m}(R)}. \quad (30)$$

These formulas follow from the standard definition of the scattering phase shifts [31].

III. SCATTERING OF UNIVERSAL DIMERS

A. Universal dimers

We consider universal dimers made of a polarised fermion of mass M and a polarised fermion of mass m . These dimers are two-body s -wave weakly-bound states. The normalised wave function $\varphi(r)$ for the relative motion of the two particles inside the dimer is given by

$$\varphi(r) = \frac{e^{-r/a}}{\sqrt{2\pi ar}}. \quad (31)$$

B. Scattering of a dimer and a particle

First, we consider the scattering of a universal dimer with a fermionic particle of mass M . To apply the RGM to this case, we set $\phi_A = \varphi$ given by Eq. (31), $\phi_B = 1$, and the interaction potential given by Eq. (17), assuming that there is no interaction between identical fermions. The antisymmetrisation operator in the calculation of the exchange potentials and kernel is obtained by considering all possible permutations of identical fermions. In this case, there

are two possibilities, as shown in Fig. 1: no permutation and the exchange of two fermions of mass M . It follows that the direct and exchange potentials of the RGM equations, Eqs. (10), and (15), are given by the following expressions:

$$V_D(\mathbf{R}) = g \left(\frac{\kappa + 1}{\kappa} \right)^3 \left| \varphi \left(\frac{\kappa + 1}{\kappa} R \right) \right|^2 \quad (32)$$

$$V_{\text{EX1}} \cdot \psi(\mathbf{R}) = g \bar{\varphi}^*(0) \varphi(R) \psi \left(-\frac{\kappa}{\kappa + 1} \mathbf{R} \right) \quad (33)$$

$$V_{\text{EX2}} \cdot \psi(\mathbf{R}) = g \bar{\varphi}(0) \left(\frac{\kappa + 1}{\kappa} \right)^3 \varphi^* \left(\frac{\kappa + 1}{\kappa} R \right) \psi \left(-\frac{\kappa + 1}{\kappa} \mathbf{R} \right), \quad (34)$$

where $\kappa = M/m$ is the mass ratio and

$$\bar{\varphi}(0) = -\lim_{r \rightarrow 0} \frac{\partial}{\partial r} r \cdot \varphi(\vec{r}) = \frac{1}{\sqrt{2\pi a a}} > 0. \quad (35)$$

The exchange kernel is given by

$$K \cdot \psi(\vec{R}) = \frac{(\kappa + 1)^6}{(1 + 2\kappa)^3} \int d^3 \mathbf{R}' \varphi^*(\mathbf{r}_1) \varphi(\mathbf{r}_2) \psi(\mathbf{R}'), \quad (36)$$

with

$$\begin{aligned} \mathbf{r}_1 &= \frac{(\kappa + 1)^2}{1 + 2\kappa} \mathbf{R}' + \frac{\kappa(\kappa + 1)}{1 + 2\kappa} \mathbf{R}, \\ \mathbf{r}_2 &= \frac{\kappa(\kappa + 1)}{1 + 2\kappa} \mathbf{R}' + \frac{(\kappa + 1)^2}{1 + 2\kappa} \mathbf{R}. \end{aligned}$$

The kinetic operator in Eqs. (10), (15) is given by

$$T_{\mathbf{R}} = -\frac{\hbar^2}{2\left(\frac{1}{M+m} + \frac{1}{M}\right)^{-1}} \nabla_{\mathbf{R}}^2.$$

The RGM1 and RGM2 equations can be solved by performing the partial-wave expansion of section II C. Here, the potentials Eqs. (32-34) do not couple partial waves:

$$V_D^{\ell m, \ell' m'} \propto \delta_{\ell, \ell'} \delta_{m, m'} \quad (37)$$

$$V_{\text{EX}}^{\ell m, \ell' m'} \propto \delta_{\ell, \ell'} \delta_{m, m'} \quad (38)$$

and for a given partial wave (ℓ, m) , we obtain from Eq. (25),

$$V_{\text{EX1}}^{\ell m, \ell m}(R, R') = (-1)^\ell g \frac{\kappa + 1}{\kappa} \bar{\varphi}^*(0) \times \varphi(R) \delta \left(R' - \frac{\kappa}{\kappa + 1} R \right), \quad (39)$$

$$V_{\text{EX2}}^{\ell m, \ell m}(R, R') = (-1)^\ell g \left(\frac{\kappa + 1}{\kappa} \right)^2 \bar{\varphi}(0) \times \varphi^* \left(\frac{\kappa + 1}{\kappa} R \right) \delta \left(R' - \frac{\kappa + 1}{\kappa} R \right). \quad (40)$$

The factor $(-1)^\ell$ in these expressions comes from the minus sign in the argument of ψ in Eqs. (33-34).

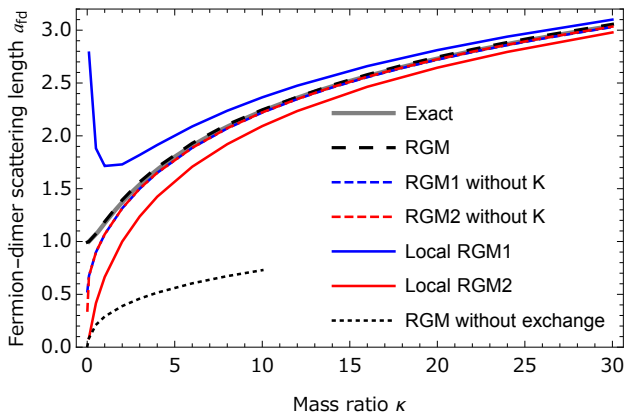


Figure 2: Fermion-dimer s -wave scattering length a_{fd} in units of a as a function of the mass ratio.

Due to this factor, the exchange potential is repulsive for even partial waves, and it is attractive for odd partial waves. Moreover, Eqs. (39-40) show that the exchange potentials have an increasingly local character as the mass ratio κ increases. Their local approximation, given by Eq. (26), leads to

$$V_{\text{EX1 local}}^{\ell m, \ell m}(R) = (-1)^\ell g \frac{\kappa + 1}{\kappa} \bar{\varphi}^*(0) \varphi(R), \quad (41)$$

$$V_{\text{EX2 local}}^{\ell m, \ell m}(R) = (-1)^\ell g \left(\frac{\kappa + 1}{\kappa} \right)^2 \bar{\varphi}(0) \varphi^* \left(\frac{\kappa + 1}{\kappa} R \right). \quad (42)$$

We solve the resulting RGM and local RGM equations numerically by discretising the coordinate R .

1. s -wave scattering

We first consider fermion-dimer scattering in the s wave, for which the effective potential is purely repulsive. The fermion-dimer s -wave scattering length a_{fd} is therefore always positive. It is shown in Fig. 2, as a function of the mass ratio κ . For the equal mass case ($M = m$), we obtain

$$a_{fd} = 1.19a,$$

which is consistent with the exact result $\approx 1.17907a$ [32, 33]. All RGM results are within 2% of the exact results, indicating that there is little excitation during the collision of a dimer and fermion, the dimer remaining bound during the collision. Nonetheless, the exchange of particles is crucial. The dotted curve in Fig. 2 shows that including only the direct potential (neglecting the exchange kernel and potential) yields a much smaller scattering length. On the other hand, the exchange kernel K brings a significant difference only for mass ratios smaller than one, and may be neglected otherwise, as shown by the dashed red and blue curves in Fig. 2. As to the local approximation, it leads to results which are close to those of the RGM for sufficiently large mass ratios, as seen from the red and blue curves in Fig. 2.

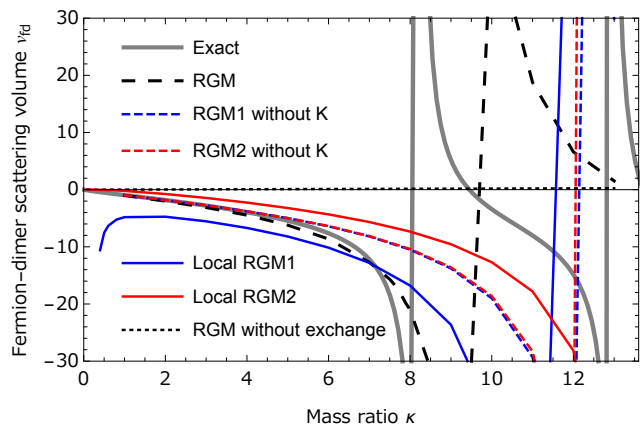


Figure 3: Fermion-dimer p -wave scattering volume v_{fd} in units of a^3 as a function of the mass ratio.

2. p -wave scattering

In the p -wave channel, the fermion and dimer attract each other. This is due to the Efimov attraction [4, 6] that results from the effective interaction between the two heavy fermions mediated by the light fermion. Although the Efimov attraction wins over the centrifugal barrier only for mass ratios $M/m > \kappa_c \approx 13.6069657$ [6, 24, 34], resulting in an infinite discrete-scale-invariant tower of three-body bound states, it also makes the system attractive for lower mass ratios, resulting in an overall negative p -wave scattering length. As the mass ratio increases, the Efimov attraction strengthens, and two universal three-body bound states appear at mass ratios $\kappa_1 = 8.17260$ and $\kappa_2 = 12.91743$ [24]. At these mass ratios, fermion-dimer p -wave scattering is resonant and the p -wave scattering volume v_{fd} diverges, as shown in Fig. 3.

In the RGM, the effective potential between the fermion and the dimer scattering in the p wave is also attractive, due to the factor $(-1)^\ell$ of Eqs. (39-40). The scattering volume calculated in the RGM is thus negative and very close to the exact one up to the mass ratio $M/m \approx 6$. For the equal mass case ($M = m$), the RGM gives

$$v_{fd} = -0.98a,$$

which is consistent with the exact result $\approx -0.96a$ [35]. Beyond the mass ratio ~ 6 , the RGM results deviate strongly from the exact results. This is explained by the fact that the resonance and the three-body bound state at $M/m = \kappa_1$ imply three-body correlations that are not fully captured by the RGM. Nevertheless, the RGM exhibits a similar resonance, but at a shifted mass ratio $\kappa_1^{(\text{RGM})} \approx 9.5$. This shows that the Efimov attraction, physically due to the exchange of light fermion between the two heavy fermions, is partially captured by the mere antisymmetrisation of the wave function in the RGM, as suggested by Fig. 1.

The local RGM equations reproduce approximately

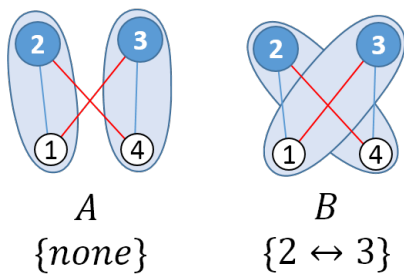


Figure 4: Schematic representation of the two permutations of identical fermions between two dimers.

the RGM results for $M/m < 6$, as shown by the blue and red curves in Fig. 3. For larger mass ratios, the difference between the local RGM and full RGM results is substantial and it is mainly due to the absence of the exchange kernel K in the local RGM equations, as shown by the dashed red and blue curves in Fig. 3.

C. Scattering of two dimers

Now, we consider the scattering of two universal dimers. We thus apply the RGM equations for the two cluster wave functions $\phi_A = \phi_B = \varphi$ given by Eq. (31) and the interaction potential given by Eq. (17), assuming again that there is no interaction between identical fermions. The antisymmetrisation operator in the calculation of the exchange potentials and kernel is obtained by considering all possible permutations of identical fermions. In this case, there are two possibilities, as shown in Fig. 4: no permutation and the exchange of two fermions of mass M (which is equivalent to exchanging the two fermions of mass m). After some straightforward calculations, the direct and exchange potentials, as well as the exchange kernel of the RGM equations, Eq. (10) and (15), are given by the following expressions:

$$V_D(\mathbf{R}) = 2g(\kappa + 1)^3 \int d^3\mathbf{r} |\varphi(\mathbf{r})\varphi((\kappa + 1)\mathbf{R} + \kappa\mathbf{r})|^2,$$

$$K(\mathbf{R}, \mathbf{R}') = -\lambda \int d^3\mathbf{r} \varphi^*(\mathbf{r} + \mathbf{R}_3) \varphi^*(\mathbf{r}) \varphi(\mathbf{r} + \mathbf{R}_1) \varphi(\mathbf{r} + \mathbf{R}_2),$$

$$V_{\text{EX1}}(\mathbf{R}, \mathbf{R}') = 2g\lambda \varphi^*(\mathbf{R}_3) \bar{\varphi}^*(0) \varphi(\mathbf{R}_1) \varphi(\mathbf{R}_2),$$

$$V_{\text{EX2}}(\mathbf{R}, \mathbf{R}') = 2g\lambda \varphi^*(\mathbf{R}_2) \varphi^*(\mathbf{R}_1) \bar{\varphi}(0) \varphi(\mathbf{R}_4).$$

In these expressions, we have set $\kappa = M/m$, $\lambda = (\kappa + 1)^6 / (2\kappa)^3$, and

$$\mathbf{R}_1 = \frac{\kappa + 1}{2\kappa} (\mathbf{R}' + \mathbf{R}),$$

$$\mathbf{R}_2 = \frac{\kappa + 1}{2} (\mathbf{R}' - \mathbf{R}),$$

$$\mathbf{R}_3 = \frac{(\kappa + 1)}{2\kappa} ((\kappa + 1)\mathbf{R}' - (\kappa - 1)\mathbf{R}),$$

$$\mathbf{R}_4 = \frac{\kappa + 1}{2\kappa} ((\kappa - 1)\mathbf{R}' - (\kappa + 1)\mathbf{R}).$$

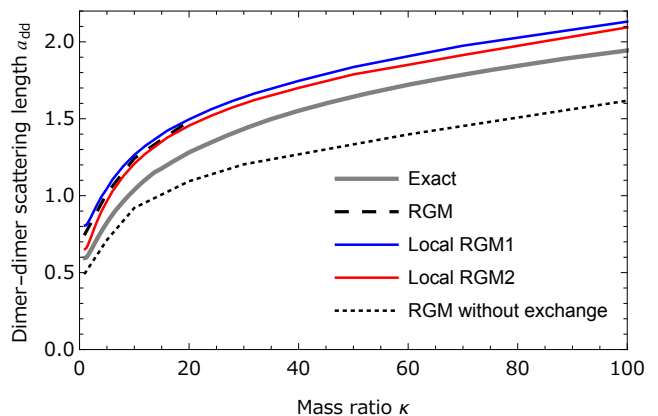


Figure 5: Dimer-dimer scattering length a_{dd} in units of a as a function of the mass ratio.

The kinetic operator in Eqs. (10), (15), (27) and (28) is given by

$$T_{\mathbf{R}} = -\frac{\hbar^2}{M + m} \nabla_{\mathbf{R}}^2. \quad (43)$$

We solve the RGM1 and RGM2 equations, as well as their local approximation, by performing the partial-wave expansion of section II C and discretising the coordinate \mathbf{R} . The potentials are repulsive for all partial waves. The resulting dimer-dimer s -wave scattering length is shown in Fig. 5, as a function of the mass ratio κ . For the equal mass case ($M = m$), we obtain

$$a_{dd} = 0.752a,$$

which is close, although significantly different, from the exact result $\approx 0.6a$ [22, 23, 36–41]. This means that compared to dimer-particle scattering, there is a bit more excitation during the collision of two dimers, although it remains small. On the other hand, exchange is less important than in the case of fermion-dimer scattering, as the major contribution to the scattering length comes from the direct potential, as seen from the dotted curve in Fig. 5. The exchange potentials have an increasingly local character as the mass ratio increases. We have calculated the scattering length with the RGM up to mass ratio 20. Beyond this mass ratio, the local character of the potential makes it difficult to solve the problem as a non-local one, since a high degree of discretisation is needed. The local RGM equations, on the other hand, are easier to solve. They give results which are very close to the RGM, as can be seen from the blue and red curves of Fig. 5, and can easily be extended to larger mass ratios.

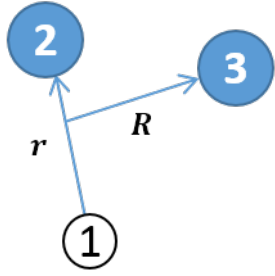


Figure 6: Jacobi coordinates \mathbf{r} and \mathbf{R} describing a trimer made of two heavy fermions and a light fermion. The vector $\mathbf{r} = \mathbf{r}_2 - \mathbf{r}_1$ is the relative position between particle 2 and 1, and the vector $\mathbf{R} = \mathbf{r}_3 - \frac{M\mathbf{r}_2 + m\mathbf{r}_1}{M+m}$ is the relative position between particle 3 and the centre of mass of particles 1 and 2.

IV. SCATTERING OF UNIVERSAL TRIMERS

A. Universal trimers

We now consider universal trimers made of two polarised fermions of mass M and a polarised fermion of mass m . Such trimers exist for a mass ratio $M/m > \kappa_1 \approx 8.17260$. They rotate with one quantum unit of angular momentum, and can therefore be in three possible internal quantum states of rotation, labelled by the quantum number $m \in \{-1, 0, 1\}$. For a mass ratio $M/m > \kappa_c \approx 13.6069657$ [6, 24, 34], the trimers are Efimov states [1, 4], characterised by the scattering length a between the two different kinds of fermions, and a three-body parameter. For a mass ratio $M/m < \kappa_c$, the trimers are Kartavtsev-Malykh states [24], characterised only by the scattering length a . We restrict our consideration to these states, and therefore to the range $\kappa_1 < M/m < \kappa_c$ where a ground-state trimer exists.

The trimer wave function is expressed as a function of Jacobi vectors \mathbf{r} and \mathbf{R} shown in Fig. 6. To a good accuracy, the trimer wave function is well approximated by the adiabatic hyperspherical form [24]

$$\phi_m(\mathbf{r}, \mathbf{R}) = \frac{f(\mathcal{R})}{\mathcal{R}^{5/2}} \left[\psi_{\text{Fad}}(\mathcal{R}, \alpha, \hat{y}) - \psi_{\text{Fad}}(\mathcal{R}, \tilde{\alpha}, \hat{y}) \right], \quad (44)$$

where the component

$$\psi_{\text{Fad}}(\mathcal{R}, \alpha, \hat{y}) = \frac{C(\mathcal{R})}{\sin 2\alpha} \psi_{\text{ang}}(\mathcal{R}, \alpha) Y_1^m(\hat{y}) \quad (45)$$

incorporates the angular momentum of the trimer through the spherical harmonic Y_1^m . The hyperangular component ψ_{ang} is given by

$$\psi_{\text{ang}}(\mathcal{R}, \alpha) = \cosh \left[s(\mathcal{R}) \left(\frac{\pi}{2} - \alpha \right) \right] - \frac{\tan \alpha}{s(\mathcal{R})} \sinh \left[s(\mathcal{R}) \left(\frac{\pi}{2} - \alpha \right) \right]. \quad (46)$$

Here, we use the following hyperspherical coordinates

$$\begin{aligned} \mathcal{R} &= \sqrt{x^2 + y^2} = \sqrt{\tilde{x}^2 + \tilde{y}^2} \\ \mathbf{x} &= \beta^{1/2} \mathbf{r} \quad \text{with } \beta = \frac{\sqrt{2\kappa+1}}{\kappa+1} \\ \mathbf{y} &= \beta^{-1/2} \mathbf{R} \end{aligned}$$

$$\begin{aligned} \tilde{\mathbf{x}} &= \sin \omega \mathbf{x} + \cos \omega \mathbf{y} \quad \text{with } \cot \omega = \frac{\sqrt{2\kappa+1}}{\kappa} \\ \tilde{\mathbf{y}} &= \cos \omega \mathbf{x} - \sin \omega \mathbf{y} \end{aligned}$$

$$\alpha = \arctan \left(\frac{x}{y} \right)$$

$$\tilde{\alpha} = \arctan \left(\frac{\tilde{x}}{\tilde{y}} \right)$$

The function $s(\mathcal{R})$ is determined by

$$\beta^{-1/2} \frac{\mathcal{R}}{a} = \frac{1+s^2}{s} \tanh \left(s \frac{\pi}{2} \right) - \frac{2}{\sin 2\omega} \frac{\cosh s\omega}{\cosh(s\frac{\pi}{2})} + \frac{\sinh s\omega}{s \sin^2 \omega \cosh(s\frac{\pi}{2})}.$$

The function $f(\mathcal{R})$ is the solution associated with the lowest eigenvalue $\varepsilon_{\text{trimer}}$ of the hyper-radial equation

$$\left[-\frac{d^2}{d\mathcal{R}^2} - \frac{s^2(\mathcal{R}) + \frac{1}{4}}{\mathcal{R}^2} - \varepsilon_{\text{trimer}} \right] f(\mathcal{R}) = 0,$$

and normalised as

$$\int_0^\infty d\mathcal{R} |f(\mathcal{R})|^2 = 1.$$

The function $C(\mathcal{R})$ is determined by the normalisation condition

$$\begin{aligned} &\frac{1}{4} \int (\sin 2\alpha)^2 d\alpha d\Omega_x d\Omega_y \times \\ &\left| \psi_{\text{Fad}}(\mathcal{R}, \alpha, \hat{y}) - \psi_{\text{Fad}}(\mathcal{R}, \tilde{\alpha}, \hat{y}) \right|^2 = 1, \end{aligned}$$

which guarantees that

$$\begin{aligned} &\int d^3\mathbf{r} d^3\mathbf{R} |\phi(\mathbf{r}, \mathbf{R})|^2 \\ &= \frac{1}{4} \int \mathcal{R}^5 d\mathcal{R} (\sin 2\alpha)^2 d\alpha d\Omega_x d\Omega_y |\phi(\mathbf{r}, \mathbf{R})|^2 \\ &= 1. \end{aligned}$$

B. Scattering of two trimers

Trimers in the same rotational state i are identical fermions and therefore scatter only in the p wave channel at low-energy. At sufficiently low energy, this p -wave scattering is negligible with respect to the s -wave scattering between trimers in different rotational

states. For this reason, we focus on the latter in this paper. There are three possible pairs of different rotational states, $\{-1, 0\}$, $\{0, 1\}$, and $\{1, -1\}$, and they all lead to the same scattering length, because of the SU(3) symmetry of this system. However, this symmetry is artificially broken by the single-channel RGM, if rotational states are given by the usual spherical harmonics. The different values of scattering lengths for the different pairs of states would thus give an indication of the error of the single-channel RGM approximation. However, a more serious issue is that spherical harmonics are complex-valued and the RGM does not ensure the scattering length to be real. To circumvent this problem, we consider an alternative basis for rotational states, which is the xyz basis formed by rotational states with angular momentum projection zero on the three axes of space. Namely,

$$Y_1^x = \frac{Y_1^1 - Y_1^{-1}}{\sqrt{2}}; \quad Y_1^y = \frac{Y_1^1 + Y_1^{-1}}{i\sqrt{2}}; \quad Y_1^z = Y_1^0.$$

In an exact calculation, it makes no difference whether one uses the usual spherical harmonics or the xyz basis, but in the case of the RGM, the xyz basis ensures the results to be real, since the wave functions in this basis are all real, and restores the SU(3) symmetry as well. This is evident if one observes that the three pairs $\{xy\}$, $\{yz\}$, and $\{zx\}$ can be transformed into each other by a rotation in space.

To apply the RGM to this scattering problem, we set $\phi_A = \phi_x$ and $\phi_B = \phi_y$ (i.e. the two clusters are two trimers in rotational state x and y). There are twelve possible permutations of identical fermions between the two trimers, as shown in Fig. 7. From this we obtain the expressions for the direct potential, the exchange potentials and the exchange kernel, which are given respectively by the following nine, six, and nine-dimensional integrals:

$$V_D(\mathbf{s}) = 2g \left(\frac{\kappa + 1}{\kappa} \right)^3 \int d^3 \mathbf{R} d^3 \mathbf{r}' d^3 \mathbf{R}' \left(|\phi_x(\mathbf{r}_-, \mathbf{R}) \phi_y(\mathbf{r}', \mathbf{R}')|^2 + |\phi_x(\mathbf{r}', \mathbf{R}') \phi_y(\mathbf{r}_+, \mathbf{R})|^2 \right) \quad (47)$$

with

$$\mathbf{r}_\pm = -\frac{\kappa + 1}{2\kappa + 1} \mathbf{R} \pm \frac{\kappa + 1}{\kappa} \mathbf{s} + \frac{\kappa + 1}{2\kappa + 1} \mathbf{R}' - \frac{1}{\kappa} \mathbf{r}' \quad (48)$$

$$\begin{aligned} V_{\text{EX1}}(\mathbf{s}, \mathbf{s}') = & g\lambda \int d^3 \mathbf{r} d^3 \mathbf{R} \left((\bar{\phi}_x(\mathbf{R}_1) \phi_y(\bar{\mathcal{R}}) \mp \bar{\phi}_y(\mathbf{R}_1) \phi_x(\mathcal{R}))^* (\phi_x(\mathcal{R}_2) \phi_y(\mathcal{R}_3) \mp \phi_y(\mathcal{R}_2) \phi_x(\mathcal{R}_3)) \right. \\ & + \frac{2}{\kappa^3} (\bar{\phi}_x(\mathbf{R}'_1) \phi_y(\mathcal{R}) \mp \bar{\phi}_y(\mathbf{R}'_1) \phi_x(\mathcal{R}))^* (\phi_x(\mathcal{R}'_2) \phi_y(\mathcal{R}'_3) \mp \phi_y(\mathcal{R}'_2) \phi_x(\mathcal{R}'_3)) \\ & \left. - \frac{2}{\kappa^3} (\phi_x(\mathcal{R}''_1) \phi_y(\mathcal{R}) \mp \phi_y(\mathcal{R}''_1) \phi_x(\mathcal{R}))^* (\phi_x(\mathcal{R}''_2) \phi_y(\mathcal{R}''_3) \mp \phi_y(\mathcal{R}''_2) \phi_x(\mathcal{R}''_3)) \right) \quad (49) \end{aligned}$$

$$\begin{aligned} V_{\text{EX2}}(\mathbf{s}, \mathbf{s}') = & g\lambda \int d^3 \mathbf{r} d^3 \mathbf{R} \left((\phi_x(\mathcal{R}_3) \bar{\phi}_y(\mathbf{R}_4) \mp \phi_y(\mathcal{R}_3) \bar{\phi}_x(\mathbf{R}_4)) (\phi_x(\mathcal{R}) \phi_y(\mathcal{R}_5) \mp \phi_y(\mathcal{R}) \phi_x(\mathcal{R}_5))^* \right. \\ & + \frac{2}{\kappa^3} (\phi_x(\mathcal{R}'_3) \bar{\phi}_y(\mathbf{R}'_4) \mp \phi_y(\mathcal{R}'_3) \bar{\phi}_x(\mathbf{R}'_4)) (\phi_x(\mathcal{R}) \phi_y(\mathcal{R}'_5) \mp \phi_y(\mathcal{R}) \phi_x(\mathcal{R}'_5))^* \\ & \left. - \frac{2}{\kappa^3} (\phi_x(\mathcal{R}''_3) \bar{\phi}_y(\mathcal{R}) \mp \phi_y(\mathcal{R}''_3) \phi_x(\mathcal{R}))^* (\phi_x(\mathcal{R}''_2) \phi_y(\mathcal{R}''_3) \mp \phi_y(\mathcal{R}''_2) \phi_x(\mathcal{R}''_3)) \right). \quad (50) \end{aligned}$$

$$\begin{aligned} K(\mathbf{s}, \mathbf{s}') = & \frac{\lambda}{4} \int d^3 \mathbf{r} d^3 \mathbf{R} d^3 \mathbf{r}' \left((\phi_x(\mathcal{R}_3) \phi_y(\mathcal{R}_4) \mp \phi_y(\mathcal{R}_3) \phi_x(\mathcal{R}_4)) (\phi_x(\mathcal{R}) \phi_y(\mathbf{r}', \mathbf{R}_5) \mp \phi_y(\mathcal{R}) \phi_x(\mathbf{r}', \mathbf{R}_5))^* \right. \\ & \left. + \frac{4}{\kappa^3} (\phi_x(\mathcal{R}'_3) \phi_y(\mathcal{R}'_4) \mp \phi_y(\mathcal{R}'_3) \phi_x(\mathcal{R}'_4)) (\phi_x(\mathcal{R}) \phi_y(\mathbf{r}', \mathbf{R}'_5) \mp \phi_y(\mathcal{R}) \phi_x(\mathbf{r}', \mathbf{R}'_5))^* \right). \quad (51) \end{aligned}$$

In these expressions, we have set

$$\bar{\phi}_m(\mathbf{R}) = -\lim_{r \rightarrow 0} \frac{\partial}{\partial r} r \phi_m(\mathbf{r}, \mathbf{R}),$$

$$\lambda = 2 \frac{(2\kappa + 1)^6}{(2\kappa)^3},$$

and \mathcal{R}_i stands for $(\mathbf{r}_i, \mathbf{R}_i)$. These variables are given explicitly in terms of \mathbf{r} and \mathbf{R} in the Appendix. The sign \mp in Eqs. (49-50) is $-$ for even scattering waves,

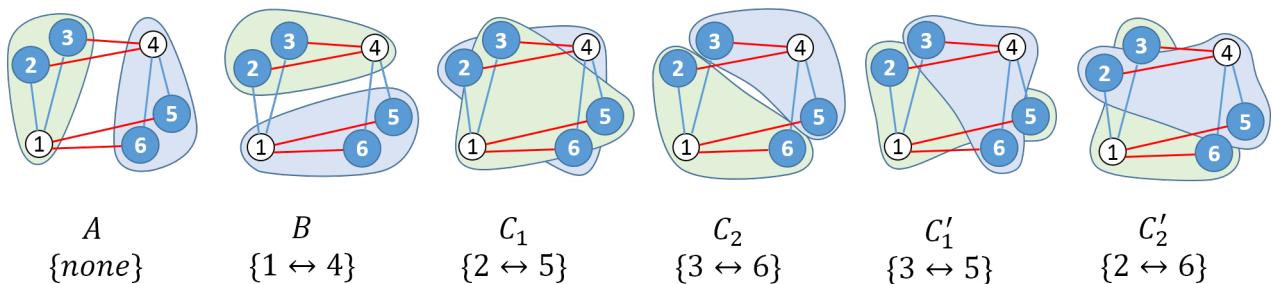


Figure 7: Schematic representation of the first six permutations of identical fermions between two trimers. The next six permutations are obtained by performing the permutation $\{1 \leftrightarrow 4, 2 \leftrightarrow 5, 3 \leftrightarrow 6\}$ (which produces a minus sign for the corresponding terms in the wave function).

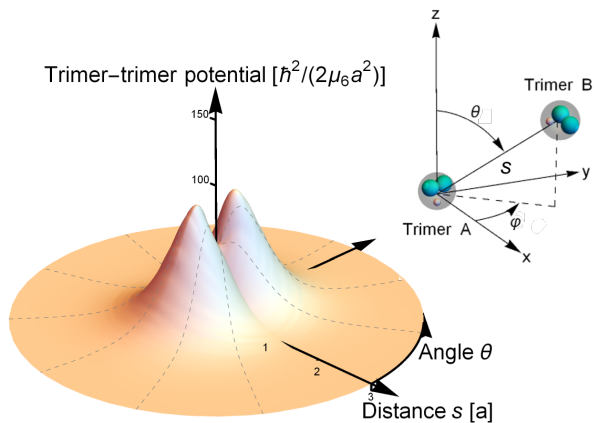


Figure 8: Integrated potential in the RGM1 - see Eq. (53) - between a trimer A in rotational state x and a trimer B in rotational state y , as a function of the distance s and angle θ (in the spherical coordinates represented in the inset) between the centres of mass of the two trimers.

and $+$ for odd scattering waves. Since we are interested in s -wave scattering, only even waves are involved due to the conservation of parity, and thus $\mp = -$ in this case. Note that the asterisk in Eqs. (49-51) still denotes the complex conjugate, although in our calculations all wave functions are real. To compute these high-dimensional integrals, we resort to Monte Carlo integration using importance sampling.

The total potential (sum of direct and exchange potentials)

$$V_1(\mathbf{s}, \mathbf{s}') = V_D(\mathbf{s})\delta^3(\mathbf{s} - \mathbf{s}') + V_{EX1}(\mathbf{s}, \mathbf{s}') \quad (52)$$

is anisotropic, due to the anisotropy of the trimers. To visualise this anisotropy, we plot in Fig. 8 the integrated potential

$$V_{I \text{ integrated}}(\mathbf{s}) = V_D(\mathbf{s}) + \int d^3 \mathbf{s}' V_{EX1}(\mathbf{s}, \mathbf{s}') \quad (53)$$

as a function of the distance s and angle θ of the spherical coordinates (s, θ, φ) - note that the potential does not depend on φ by rotational symmetry along the z axis. Fig. 8 shows that the anisotropy of the potential is moderate. As a result, we only need to consider the

partial waves $\ell = 0$ and $\ell = 2$ to get converged results. Fig. 8 also indicates that the potential is repulsive. This fact is confirmed by the numerical calculation of the potential in each partial wave given by Eqs. (23-25). As a result, the trimer-trimer s -wave scattering is positive.

We have found that the exchange potentials are to a good approximation local potentials. In view of the previous results for dimers, we substitute the exchange potential by their local approximation given by Eqs. (25) and (26) and neglect the exchange kernel, which is costly to evaluate. We therefore use the local RGM1 and RGM2 equations, Eqs. (27-28).

The resulting trimer-trimer s -wave scattering length is plotted in Fig. 9 as a function of the mass ratio κ . The results are similar to the dimer-dimer case. As in the dimer-dimer case, the local RGM1 and RGM2 results are very close, suggesting that the local approximation is enough to reproduce the RGM, and the contribution from the exchange of particles is small compared to the direct contribution. However, unlike the dimer-dimer case, the scattering length decreases with the mass ratio. This is due to the fact that the binding energy of the trimers increases, and thus their size reduces, as the mass ratio increases.

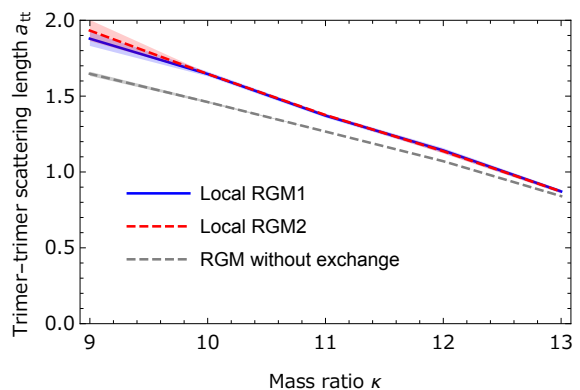


Figure 9: Trimer-trimer scattering length a_{tt} in units of a as a function of the mass ratio, calculated by the local RGM1 and RGM2. The shaded area indicates the statistical uncertainty due to the Monte Carlo integration used to calculate the potentials.

The decrease of the scattering length is therefore a consequence of the decrease of the scattering cross section, due to the decreased size of the trimers.

V. CONCLUSION

We have applied the resonating group method to the scattering of universal clusters which are described by zero-range interactions. We have found that the single-channel RGM is relevant to clusters made of fermions. It reproduces qualitatively, and in some limits quantitatively, the exact results for scattering involving universal dimers. We have also applied the single-channel RGM to the scattering of universal trimers. It is found to be similar to the scattering of dimers: there is little contribution from the exchange of particles and the effective interaction is repulsive, unlike the scattering of a fermion and a dimer, where exchange is dominant and produces attraction related to the Efimov effect. As a consequence, we obtain a positive trimer-trimer s -wave scattering length. This result has implications for the nature and stability of the ground state of a mixture of heavy and light fermions which are to be discussed in a separate work.

The validity and accuracy of the present RGM cal-

culations are limited by the single-channel approximation. In particular, it is likely that trimers excite into the nearby dimer-particle continuum during their collision, by analogy with nuclear systems where excited channels play an important role [42]. Including these extra channels, i.e. states of the form Eq. (1) constructed with other eigenstates of the n -body and $N - n$ -body subsystems, should converge to the exact results. It remains however numerically challenging to go beyond the single-channel approximation for clusters of more than two particles. As it stands, the single-channel RGM can already give useful insights on the interactions between universal clusters. It could be used to further investigate similar problems, such as scattering of dimers and trimers, involving unpolarised fermions or three-component fermions.

Acknowledgments: The authors are grateful to Tet-suo Hatsuda, Vojtěk Krejčířík, Eite Tiesinga, and Sofia Quaglioni for helpful discussions. P. N. acknowledges support from RIKEN through the Incentive Research Project funding. S. E. acknowledges support from JSPS. A. M. G. was supported by EPSRC, grant No. EP/I004637/1, FCT, grant PTDC/FIS/111348/2009 and a Marie Curie International Reintegration Grant PIRG07-GA-2010-268172.

-
- [1] E. Braaten and H.-W. Hammer, *Physics Reports* **428**, 259 (2006), ISSN 0370-1573, URL <http://www.sciencedirect.com/science/article/pii/S0370157306000822>.
- [2] J. Wang, J. D’Incao, B. Esry, and C. Greene, *Phys. Rev. Lett.* **108**, 263001 (2012), URL <http://link.aps.org/doi/10.1103/PhysRevLett.108.263001>.
- [3] P. Naidon, S. Endo, and M. Ueda, *Phys. Rev. A* **90**, 022106 (2014), URL <http://link.aps.org/doi/10.1103/PhysRevA.90.022106>.
- [4] V. Efimov, *Yad. Fiz.* **12**, 1080 (1970), [*Sov. J. Nucl. Phys.* **12**, 589-595 (1971)].
- [5] V. Efimov, *Physics Letters B* **33**, 563 (1970), ISSN 0370-2693, URL <http://www.sciencedirect.com/science/article/pii/0370269370903497>.
- [6] V. Efimov, *Nuclear Physics A* **210**, 157 (1973), ISSN 0375-9474, URL <http://www.sciencedirect.com/science/article/pii/0375947473905101>.
- [7] J. Herbig, T. Kraemer, M. Mark, T. Weber, C. Chin, H.-C. Nägerl, and R. Grimm, *Science* **301**, 1510 (2003), <http://www.sciencemag.org/content/301/5639/1510.full.pdf>, URL <http://www.sciencemag.org/content/301/5639/1510.abstract>.
- [8] C. A. Regal, C. Ticknor, J. L. Bohn, and D. S. Jin, *Nature* **424**, 47 (2003), URL <http://dx.doi.org/10.1038/nature01738>.
- [9] S. Dürr, T. Volz, A. Marte, and G. Rempe, *Phys. Rev. Lett.* **92**, 020406 (2004), URL <http://link.aps.org/doi/10.1103/PhysRevLett.92.020406>.
- [10] J. Cubizolles, T. Bourdel, S. J. J. M. F. Kokkelmans, G. V. Shlyapnikov, and C. Salomon, *Phys. Rev. Lett.* **91**, 240401 (2003), URL <http://link.aps.org/doi/10.1103/PhysRevLett.91.240401>.
- [11] S. Jochim, M. Bartenstein, A. Altmeyer, G. Hendl, C. Chin, J. H. Denschlag, and R. Grimm, *Phys. Rev. Lett.* **91**, 240402 (2003), URL <http://link.aps.org/doi/10.1103/PhysRevLett.91.240402>.
- [12] K. E. Strecker, G. B. Partridge, and R. G. Hulet, *Phys. Rev. Lett.* **91**, 080406 (2003), URL <http://link.aps.org/doi/10.1103/PhysRevLett.91.080406>.
- [13] M. W. Zwierlein, C. A. Stan, C. H. Schunck, S. M. F. Raupach, S. Gupta, Z. Hadzibabic, and W. Ketterle, *Phys. Rev. Lett.* **91**, 250401 (2003), URL <http://link.aps.org/doi/10.1103/PhysRevLett.91.250401>.
- [14] C. Ospelkaus, S. Ospelkaus, L. Humbert, P. Ernst, K. Sengstock, and K. Bongs, *Phys. Rev. Lett.* **97**, 120402 (2006), URL <http://link.aps.org/doi/10.1103/PhysRevLett.97.120402>.
- [15] T. Kraemer, M. Mark, P. Waldburger, J. G. Danzl, C. Chin, B. Engeser, A. D. Lange, K. Pilch, A. Jaakkola, H.-C. Nägerl, et al., *Nature* **440**, 315 (2006), URL <http://dx.doi.org/10.1038/nature04626>.
- [16] T. Lompe, T. B. Ottenstein, F. Serwane, A. N. Wenz, G. Zürn, and S. Jochim, *Science* **330**, 940 (2010), <http://www.sciencemag.org/content/330/6006/940.full.pdf>, URL <http://www.sciencemag.org/content/330/6006/940.abstract>.
- [17] S. Nakajima, M. Horikoshi, T. Mukaiyama, P. Naidon, and M. Ueda, *Phys. Rev. Lett.* **106**, 143201 (2011), URL <http://link.aps.org/doi/10.1103/PhysRevLett.106.143201>.
- [18] J. von Stecher, J. P. D’Incao, and C. H. Greene, *Nature Physics* **5**, 417 (2009), URL <http://dx.doi.org/10.1038/nphys1253>.

- [19] J. von Stecher, Journal of Physics B: Atomic, Molecular and Optical Physics **43**, 101002 (2010), URL <http://stacks.iop.org/0953-4075/43/i=10/a=101002>.
- [20] D. Blume, Phys. Rev. Lett. **109**, 230404 (2012), URL <http://link.aps.org/doi/10.1103/PhysRevLett.109.230404>.
- [21] F. Ferlaino, S. Knoop, M. Berninger, W. Harm, J. D’Incao, H.-C. Nägerl, and R. Grimm, Phys. Rev. Lett. **102**, 140401 (2009), URL <http://link.aps.org/doi/10.1103/PhysRevLett.102.140401>.
- [22] D. S. Petrov, C. Salomon, and G. V. Shlyapnikov, Phys. Rev. Lett. **93**, 090404 (2004), URL <http://link.aps.org/doi/10.1103/PhysRevLett.93.090404>.
- [23] B. Marcellis, S. J. J. M. F. Kokkelmans, G. V. Shlyapnikov, and D. S. Petrov, Phys. Rev. A **77**, 032707 (2008), URL <http://link.aps.org/doi/10.1103/PhysRevA.77.032707>.
- [24] O. I. Kartavtsev and A. V. Malykh, Journal of Physics B: Atomic, Molecular and Optical Physics **40**, 1429 (2007), URL <http://stacks.iop.org/0953-4075/40/i=7/a=011>.
- [25] J. A. Wheeler, Phys. Rev. **52**, 1083 (1937), URL <http://link.aps.org/doi/10.1103/PhysRev.52.1083>.
- [26] D. Thompson, M. LeMere, and Y. Tang, Nuclear Physics A **286**, 53 (1977).
- [27] Y.-C. Tang, M. LeMere, and D. Thompson, Physics Reports **47**, 167 (1978).
- [28] A. Faessler, Progress in particle and nuclear physics **11**, 171 (1984).
- [29] K. Shimizu, Reports on Progress in Physics **52**, 1 (1989).
- [30] M. Oka, K. Shimizu, and K. Yazaki, Progress of Theoretical Physics Supplement **137**, 1 (2000).
- [31] F. Calogero, *Variable Phase Approach to Potential Scattering* (Elsevier Science, 1967).
- [32] G. Skorniakov and K. Ter-Martirosian, Sov. Phys. JETP **4**, 648 (1957).
- [33] M. Iskin, Phys. Rev. A **81**, 043634 (2010), URL <http://link.aps.org/doi/10.1103/PhysRevA.81.043634>.
- [34] D. S. Petrov, Phys. Rev. A **67**, 010703 (2003), URL <http://link.aps.org/doi/10.1103/PhysRevA.67.010703>.
- [35] S. Endo, P. Naidon, and M. Ueda, Few-Body Systems pp. DOI: 10.1007/s00601-011-0229-6 (2011).
- [36] G. E. Astrakharchik, J. Boronat, J. Casulleras, Giorgini, and S., Phys. Rev. Lett. **93**, 200404 (2004), URL <http://link.aps.org/doi/10.1103/PhysRevLett.93.200404>.
- [37] D. S. Petrov, C. Salomon, and G. V. Shlyapnikov, Phys. Rev. A **71**, 012708 (2005), URL <http://link.aps.org/doi/10.1103/PhysRevA.71.012708>.
- [38] D. S. Petrov, C. Salomon, and G. V. Shlyapnikov, Journal of Physics B: Atomic, Molecular and Optical Physics **38**, S645 (2005), URL <http://stacks.iop.org/0953-4075/38/i=9/a=014>.
- [39] I. V. Brodsky, M. Y. Kagan, A. V. Klaptsov, R. Combescot, and X. Leyronas, Phys. Rev. A **73**, 032724 (2006), URL <http://link.aps.org/doi/10.1103/PhysRevA.73.032724>.
- [40] J. Levinsen and V. Gurarie, Phys. Rev. A **73**, 053607 (2006), URL <http://link.aps.org/doi/10.1103/PhysRevA.73.053607>.
- [41] J. von Stecher, C. H. Greene, and D. Blume, Phys. Rev. A **76**, 053613 (2007), URL <http://link.aps.org/doi/10.1103/PhysRevA.76.053613>.
- [42] G. Hupin, J. Langhammer, P. Navrátil, S. Quaglioni, A. Calci, and R. Roth, Phys. Rev. C **88**, 054622 (2013), URL <http://link.aps.org/doi/10.1103/PhysRevC.88.054622>.

VI. APPENDIX

Here we give the explicit expressions for the variables appearing in Eqs. (49) and (50).

For Eq. (49) we have:

$$\mathbf{R}_1 = \frac{(2\kappa+1)(2\kappa-1)}{2\kappa} \mathbf{s} - \frac{(2\kappa+1)^2}{2\kappa} \mathbf{s}' + \frac{2\kappa+1}{\kappa+1} \mathbf{r} + \mathbf{R}$$

$$\mathbf{r}_2 = \left(\kappa + \frac{1}{2}\right) (\mathbf{s}' - \mathbf{s})$$

$$\mathbf{R}_2 = \frac{(1+2\kappa)(2\kappa^2-1)}{2\kappa(1+\kappa)} \mathbf{s} - \frac{(1+2\kappa)(2\kappa^2+2\kappa+1)}{2\kappa(1+\kappa)} \mathbf{s}' + \frac{1+2\kappa}{1+\kappa} \mathbf{r} + \mathbf{R}$$

$$\mathbf{r}_3 = \left(\kappa + \frac{1}{2}\right) (\mathbf{s} - \mathbf{s}') + \mathbf{r}$$

$$\mathbf{R}_3 = \frac{1+2\kappa}{2(1+\kappa)} (\mathbf{s} - \mathbf{s}') + \mathbf{R}$$

$$\mathbf{R}'_1 = \frac{2\kappa+1}{2\kappa^2} \mathbf{s} - \frac{(2\kappa+1)^2}{2\kappa^2} \mathbf{s}' - \frac{2\kappa+1}{\kappa(\kappa+1)} \mathbf{r} + \mathbf{R}$$

$$\mathbf{r}'_2 = \left(1 + \frac{1}{2\kappa}\right) (\mathbf{s} - \mathbf{s}')$$

$$\mathbf{R}'_2 = \frac{(1+\kappa-\kappa^2)(1+2\kappa)}{2\kappa^2(1+\kappa)} \mathbf{s} - \frac{(1+2\kappa)(\kappa^2+3\kappa+1)}{2\kappa^2(1+\kappa)} \mathbf{s}' - \frac{1+2\kappa}{(1+\kappa)\kappa} \mathbf{r} + \mathbf{R}$$

$$\mathbf{r}'_3 = \left(1 + \frac{1}{2\kappa}\right) (\mathbf{s}' - \mathbf{s}) + \mathbf{r}$$

$$\mathbf{R}'_3 = \frac{1+2\kappa}{2(1+\kappa)} (\mathbf{s} - \mathbf{s}') + \mathbf{R} \equiv \mathbf{R}_3$$

$$\mathbf{r}''_1 = -\left(1 + \frac{1}{2\kappa}\right) (\mathbf{s} - \mathbf{s}') + \frac{1}{1+\kappa} \mathbf{r} - \mathbf{R}$$

$$\mathbf{R}''_1 = -\frac{1+2\kappa}{2\kappa(1+\kappa)} \mathbf{s} - \frac{(1+2\kappa)^2}{2\kappa(1+\kappa)} \mathbf{s}' - \frac{1+2\kappa}{(1+\kappa)^2} \mathbf{r} - \frac{1+\kappa-\kappa^2}{\kappa(1+\kappa)} \mathbf{R}$$

$$\mathbf{r}''_2 = \frac{1}{1+\kappa} \mathbf{r} - \mathbf{R}$$

$$\mathbf{R}''_2 = -\left(1 + \frac{1}{2\kappa}\right) (\mathbf{s} + \mathbf{s}') - \frac{1+2\kappa}{(1+\kappa)^2} \mathbf{r} - \frac{1+\kappa-\kappa^2}{\kappa(1+\kappa)} \mathbf{R}$$

$$\mathbf{r}''_3 = \left(1 + \frac{1}{2\kappa}\right) (\mathbf{s}' - \mathbf{s}) + \mathbf{r} \equiv \mathbf{r}'_3$$

$$\mathbf{R}''_3 = \frac{1+2\kappa}{2(1+\kappa)} (\mathbf{s} - \mathbf{s}') + \mathbf{R} \equiv \mathbf{R}'_3 \equiv \mathbf{R}_3$$

Note that $\mathbf{R}_3'' = \mathbf{R}_3' = \mathbf{R}_3$ and $\mathbf{r}_3'' = \mathbf{r}_3'$.
 Additionally, for Eq. (50) we have:

$$\begin{aligned}\mathbf{R}_4 &= -\mathbf{R} - \frac{1+2\kappa}{1+\kappa}\mathbf{r} + \left(1 + \frac{1}{2\kappa}\right)(\mathbf{s} + \mathbf{s}') \\ \mathbf{r}_5 &= -\left(\kappa + \frac{1}{2}\right)(\mathbf{s} - \mathbf{s}') \\ \mathbf{R}_5 &= -\frac{(2\kappa+1)}{\kappa+1}\mathbf{r} - \mathbf{R} + \frac{(2\kappa+1)^2}{2\kappa(\kappa+1)}\mathbf{s}' + \frac{(2\kappa+1)}{2\kappa(\kappa+1)}\mathbf{s} \\ \\ \mathbf{R}_4' &= \mathbf{R} - \frac{1+2\kappa}{(1+\kappa)\kappa}\mathbf{r} - \left(1 + \frac{1}{2\kappa}\right)(\mathbf{s} + \mathbf{s}') \\ \mathbf{r}_5' &= -\left(1 + \frac{1}{2\kappa}\right)(\mathbf{s} - \mathbf{s}') \\ \mathbf{R}_5' &= -\frac{(2\kappa+1)}{\kappa(\kappa+1)}\mathbf{r} + \mathbf{R} - \frac{(2\kappa+1)^2}{2\kappa(\kappa+1)}\mathbf{s}' - \frac{(2\kappa+1)}{2\kappa(\kappa+1)}\mathbf{s}\end{aligned}$$

And for Eq. (51) we have:

$$\begin{aligned}\mathbf{r}_4 &= \mathbf{r}' + \left(\kappa + \frac{1}{2}\right)(\mathbf{s} - \mathbf{s}') \\ \mathbf{r}_4' &= \mathbf{r}' + \left(1 + \frac{1}{2\kappa}\right)(\mathbf{s} - \mathbf{s}')\end{aligned}$$